scientific reports

OPEN

CD200R1 modulates myelin phagocytosis and spleen response following spinal cord injury

Bruno Pannunzio[1,2], Fabio Andrés Cawen[1,3,4], Frances Evans[1,2], Rubèn López-Vales[5,6], Hugo Peluffo[1,3,4] & Natalia Lago[1,5,6]✉

The interaction between CD200 and its receptor CD200R1 plays a key role in modulating immune responses in nervous system disorders. This study explored the function of CD200R1 in local and systemic inflammation following spinal cord injury (SCI) using CD200R1-knockout (CD200R1$^{-/-}$) mice. Following a low thoracic contusion injury, CD200R1$^{-/-}$ mice exhibited increased macrophage infiltration at the injury site, with a greater proportion of pro-inflammatory Ly6C + macrophages. Myelin phagocytosis was impaired in CD200R1$^{-/-}$ macrophages both ex vivo and in vitro, indicating a reduced capacity to clear myelin debris. Despite these immune alterations, CD200R1 deficiency did not affect spontaneous locomotor recovery post-SCI, as measured by the Basso Mouse Scale. However, CD200R1$^{-/-}$ mice tended to lose more weight after injury, suggesting systemic effects. In uninjured (naïve) conditions, CD200R1$^{-/-}$ mice showed reduced spleen weight and lymphocyte counts, along with lower mRNA expression of inflammatory cytokines TNFα, IL6, and CCL2, though no significant differences were seen in splenic immune cell populations. Altogether, these results suggest that CD200R1 is an important factor regulating myelin phagocytosis by macrophages and maintaining normal immune and splenic homeostasis under both injured and naïve conditions.

Keywords Spinal cord injury, CD200R1, Myelin phagocytosis, Spleen, Inflammation

In recent years, immune receptors have been highlighted to play a role in brain and systemic homeostasis and during inflammatory conditions. Immune receptors, defined as receptors present in immune cells, have been shown to interact with different cell populations in order to maintain a homeostatic milieu and to respond in front of different pathological conditions to recover homeostasis in injured or infected tissues, including the nervous system.

Among the different immune receptors that have been highlighted, CD200R1 has been described as an important partner in modulating restraining signals in homeostasis, playing a crucial role in regulating immune responses[1]. CD200R1 is one of the 5 members of the CD200R receptor family described in mice[2]. Among the studied isoforms, CD200R1 is the most characterized, as it has been shown to have the highest affinity for the CD200 protein, its ligand in mice and humans[2].

The members of the CD200R family are predominantly expressed in myeloid cells, such as macrophages, microglia, dendritic cells, and granulocytes, as well as in subsets of lymphocytes, including natural killer (NK) cells and B and T lymphocytes[3–5]. Additionally, the expression of these receptors has been reported in certain subtypes of astrocytes and oligodendrocytes in the Central Nervous System (CNS)[4,6,7]. Their expression patterns may vary depending on the cell type and differentiation status.

CD200R1 has several unique features that make it unusual compared to most inhibitory immune receptors, which typically have an immunoreceptor tyrosine-based inhibitory motif (ITIM) in their cytoplasmic domain that recruits phosphatases once activated. In contrast, CD200R1 contains phosphotyrosine motifs in its cytoplasmic domain, which recruit the adaptors DOK1/DOK2 and RasGap[8]. These adaptors promote the inhibition of the Ras-ERK and PI3K signalling pathways. As a result of this pathway inhibition, there is a reduction in the

[1]Institut Pasteur de Montevideo, Montevideo, Uruguay. [2]Histology and Embryology Department, Faculty of Medicine, Universidad de la República, Montevideo, Uruguay. [3]Unitat de Bioquímica i Biologia Molecular, Departament de Biomedicina, Facultat de Medicina i Ciències de la Salut, Universitat de Barcelona (UB), Barcelona 08036, Spain. [4]Institut de Neurociències, Universitat de Barcelona (UB), Barcelona 08036, Spain. [5]Departament de Biologia Cel·lular, Fisiologia i Immunologia, Institut de Neurociències, Universitat Autònoma de Barcelona, Bellaterra 08193, Spain. [6]Centro de Investigación Biomédica en Red sobre Enfermedades Neurodegenerativas (CIBERNED), Madrid, Spain. ✉email: Natalia.Lago@uab.cat

production of pro-inflammatory signals through the downregulation of the NF-κB pathway[9]. Although the effect on the NF-κB pathway has been demonstrated, other unknown pathways may also be involved.

After studies reporting the presence of CD200 in lymphoid and nervous tissues, as well as the expression of CD200R1 in major immune cell populations, the interaction between CD200 and CD200R1 was quickly suggested as a potentially significant factor in regulating immune responses throughout the body. The widespread expression of CD200 is a significant advantage, as it allows the organism to locally regulate immune activity and inflammation levels. The ability of the pair CD200-CD200R1 to act as an immune checkpoint comes from cancer studies showing that the overexpression of CD200 by tumour cells can act as an immune escape mechanism by suppressing the immune response against cancer[10,11] and transplants[12,13]. Therefore, CD200R1 is considered to trigger don't eat me signals and anti-inflammatory actions.

In the CNS, CD200 is expressed mainly by neurons and endothelial cells in the CNS[3,14] and together, the pair CD200-CD200R1 has been described to mediate microglial restraining signals[15] and a "non-eat me signal" in homeostasis[16]. One of the first studies demonstrating the importance of the pair CD200-CD200R1 showed that in the absence of CD200, microglial cells displayed an inflammatory phenotype[17]. After this study, several studies pointed out the importance of this immune receptor modulating different aspects of pathologies such as multiple sclerosis, aging, stroke and spinal cord injury (SCI), among others[18–22]. Some of these studies demonstrated a role of CD200-CD200R1 interaction in the development of the local inflammatory response at the injury site, limiting inflammation and the progression of damage to nervous tissue. However, all these conditions are known to produce systemic effects, in particular in immune organs like the spleen, and no data is available regarding the role of CD200R1 in these processes.

In the context of SCI, the CD200-CD200R1 interaction has been shown to constitute a key factor regulating myeloid cells at the spinal cord level. Using CD200-knockout mice Cohen and colleagues conducted a study highlighting the significance of the CD200 ligand present in endothelial cells formed after injury and regulating the recruitment of myeloid cells after SCI[21]. Later, the study conducted by Lago and colleagues showed that inhibiting CD200R1 signalling with a blocking antibody, led to impaired recovery of locomotor functions, accompanied by an exacerbated inflammatory response and increased nervous tissue loss[22]. Conversely, activating the receptor with an agonist improved functional recovery, highlighting the neuroprotective role of the receptor and emphasizing the critical role of the CD200-CD200R1 interaction[22]. Surprisingly, the inhibition of CD200R1 with blocking antibodies after peripheral nerve injury led to delayed regeneration and decreased local inflammation[23]. Thus, the role of CD200R1 under acute traumatic injuries to the nervous system remains not well understood, with no data available regarding its involvement in key related processes such as the phagocytosis and clearance of myelin debris. Moreover, the broader role of CD200-CD200R1 interaction in the development of both local and in whole-organism inflammatory response has not been studied.

Since CD200R1 has been widely recognized as an immunomodulatory receptor involved in regulating inflammation across various pathologies, in the present study we aim to evaluate the role of CD200R1 not only in the local inflammatory response but also in systemic immune regulation, particularly focusing on its involvement in the spleen's response following SCI since, beyond its established functions in immune surveillance and blood filtration[24], the spleen is a major source of monocytes recruited to the spinal cord parenchyma after SCI[25,26].

Our findings revealed that although CD200R1 deficiency did not significantly affect functional recovery after SCI, it disrupted normal myelin phagocytosis and led to subtle alterations in monocyte recruitment. Furthermore, the absence of CD200R1 caused splenic atrophy, both in naïve conditions and after SCI, along with decreased cytokine levels, impairing the spleen's normal inflammatory response. These results underscore the critical role of CD200R1 in regulating both local and systemic inflammatory processes following SCI.

Results

CD200R1 modulates acute macrophage infiltration in the spinal cord after injury

Local and transient CD200R1 inhibition after SCI has been shown to be detrimental for locomotor recovery[22]. To understand the role of global and long-term CD200R1 inhibition in SCI, we performed a contusion to the spinal cord to WT and CD200R1$^{-/-}$ female mice. This traumatic injury elicits robust local inflammation within the central nervous system (CNS) and leads to the release of damage-associated molecular patterns (DAMPs) into circulation, consequently influencing the spleen and other organs[27]. It has been reported that the transient blocking of the interaction between CD200 and CD200R1 by using a blocking antibody against CD200R1, led to a more pro-inflammatory milieu evidenced by a higher iNOS and Ly6C markers expression in microglia and macrophages[22]. To further understand the role of the receptor in neuroinflammatory processes, we here evaluated the dynamics of microglial cells and the main immune cell populations infiltrated locally at the spinal cord after injury such as macrophages and neutrophils (Fig. 1A). Spinal cord dissection and processing for flow cytometry showed no differences neither in the number of microglial cells nor in the number of neutrophils recruited from blood (Fig. 1B-C; Suppl. Figure 2) at the different time points studied between both genotypes. Moreover, there were no differences in lymphocytes recruited into the spinal cord parenchyma at 14 dpi between genotypes (Suppl. Figure 3). Interestingly, the number of CD45^{high} and F4/80^{+} macrophages (or strongly activated microglia) at the injury site increased by the absence of CD200R1, acutely at 24 h post-SCI. (Fig. 1D). Furthermore, 24 h after the injury, the proportion of Ly6C macrophage population in CD200R1$^{-/-}$ mice was higher than in WT mice (Fig. 1E). These alterations were not observed at 3 and 7 dpi.

Myelin phagocytosis is impaired on CD200R1$^{-/-}$ macrophages

One of the pivotal roles of infiltrating immune cells and resident microglia in the context of neuroinflammation, particularly following a SCI, is their engagement in the phagocytosis of cellular debris, notably targeting myelin for clearance. Previous studies have shown that CD200R1 may be implicated in the regulation of phagocytosis of amyloid peptides[28]. However, it is still unclear whether CD200R1 plays a role in regulating myelin phagocytosis

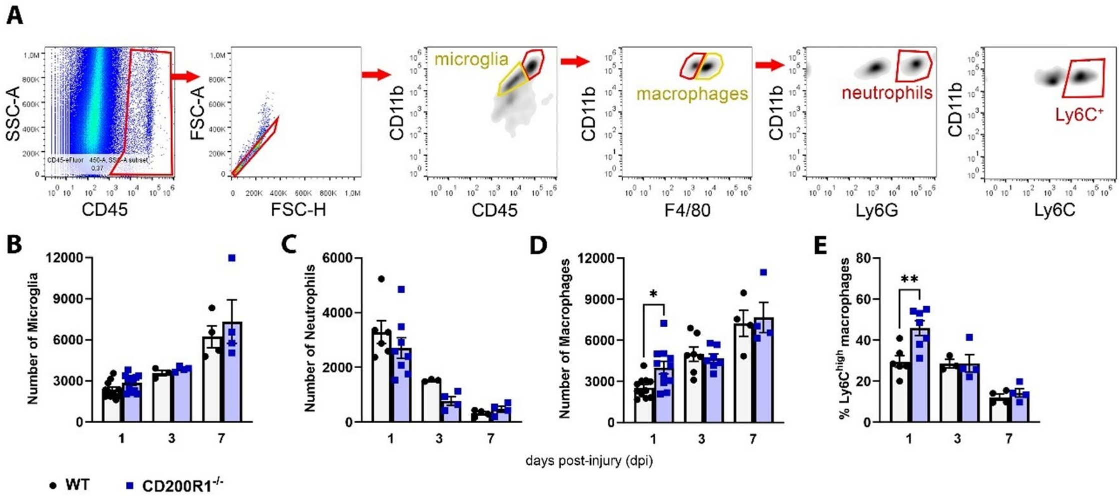

Fig. 1. CD200R1$^{-/-}$ mice exhibit increased macrophage numbers acutely after SCI. (**A**) Representative flow cytometry dot blots and density plots of injured spinal cord showing the gating for microglia, macrophages and neutrophils identification 24 h after SCI. (**B**–**E**) Quantitative analysis of: (**B**) microglial cells, (**C**) neutrophils and (**D**) macrophages in the spinal cord at different days post injury (dpi). In (**E**) proportion of Ly6C$^+$ macrophages. Each symbol represents one animal. Data are presented as mean ± SEM. Statistical analysis: Two-way ANOVA followed by Bonferroni post-hoc test, *$p \leq 0.05$, **$p \leq 0.01$.

following SCI. Thus, we assessed whether the absence of CD200R1 affects the regulation of myelin debris phagocytosis by immune cells, both at the injury site and in vitro. First, we analysed the phagocytic activity of microglia, neutrophils and macrophages from the injured spinal cord at 1, 3 and 7 dpi. After harvesting the spinal cord and performing enzymatic and mechanical disaggregation, total cells were directly incubated for 4 h with myelin conjugated to the fluorescent probe pHrodo (Fig. 2A, B). We observed no significant impact of the absence of CD200R1 in the presence of pHrodo-myelin in microglial cells (Fig. 2C) and neutrophils (Suppl. Figure 4) at 1, 3 and 7 dpi. However, 24 h after injury, we observed a lower proportion of macrophages isolated from CD200R1$^{-/-}$ mice showing intracelullar pHrodo-labeled myelin compared to the macrophage population obtained from the spinal cord of WT mice (Fig. 2D). No differences were observed in the normalized median fluorescence intensity (MFI) (Suppl. Figure 2B), i.e. the quantity of myelin phagocytosed per cell. These data suggest that, although more macrophages infiltrated and greater proportion of them were Ly6C$^+$ in CD200R1$^{-/-}$ mice, these macrophages have less phagocytic activity than those from WT mice at the injury site. We further confirmed the ex vivo results by an in vitro assay of myelin phagocytosis using bone-marrow derived macrophages (BMDMs) from WT and CD200R1$^{-/-}$ mice (Fig. 2E,F). In basal conditions without any stimuli, we observed a reduced phagocytosis of pHrodo-labeled myelin in CD200R1$^{-/-}$ BMDMs compared to WT BMDMs, both in terms of proportion of pHrodo$^+$ cells (Fig. 2G) and normalized MFI per cell (Fig. 2H). We also evaluated the phagocytosis in the presence of LPS, to test the role of CD200R1 in myelin phagocytosis under inflammatory conditions. As described previously[29,30], we observed a decreased phagocytic activity in WT BMDMs treated with LPS, but CD200R1$^{-/-}$ BMDMs pHrodo-labeled myelin phagocytic activity was unaltered in the presence of LPS (Fig. 2G, H). This suggests a relevant role of CD200R1 in regulating myelin phagocytosis, independently of the presence of an inflammatory stimulus.

Functional outcome and weight loss in CD200R1$^{-/-}$ mice after spinal cord injury

Next, we assessed whether the increase in Ly6C$^+$ macrophages and the lower myelin phagocytosis capability of macrophages lacking CD200R1, had a significant impact on the spontaneous functional recovery after SCI. Locomotor function was evaluated until 28 days post-injury (dpi) by using the Basso Mouse Scale (BMS). We did not find a significant difference in the recovery of function of mice lacking CD200R1 in comparison with WT mice (Fig. 3B). Moreover, we found a similar area of spared myelin in absence of CD200R1 at 28 dpi (Fig. 3C) suggesting that the impairment in myelin phagocytosis had not a gross impact in demyelination after SCI. Intriguingly, when we followed the body weight loss after SCI, we did find a trend towards long-lasting enhanced weight loss after the SCI in animals lacking CD200R1 in comparison with WT mice (Fig. 3D). To further understand if there was a significant and long-lasting effect on the % of weight loss, we pooled together all data available of % weight loss at 28 dpi and again only found a trend ($p = 0.09$) towards an increased weight loss in CD200R1$^{-/-}$ mice (Fig. 3E).

The observations in body weight loss after SCI, although mild, could indicate a putative influence of CD200R1 deficiency on systemic processes, potentially disrupting the physiological response of essential organs towards inflammatory stimuli, notably those integral to immune regulation. Consequently, we conducted a comprehensive analysis of immune responses within pivotal organs orchestrating and contributing to immunological modulation, including the bloodstream and the spleen.

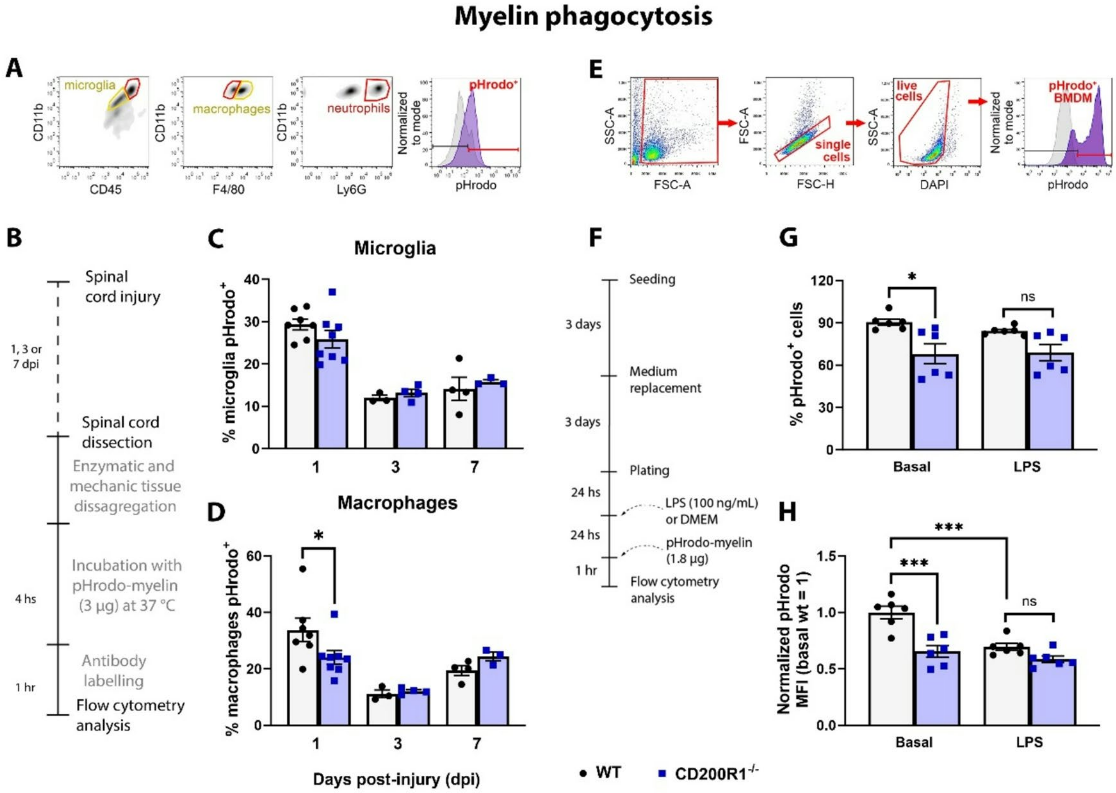

Fig. 2. Myelin phagocytosis is altered in macrophages lacking CD200R1. (**A**,**B**) Gating strategy (continued from Fig. 1A) and flow cytometry assay scheme of pHrodo-myelin phagocytosis by cell populations obtained from the spinal cord tissue after injury. (**C**) Percentage of pHrodo$^+$ microglia at 1, 3 and 7 days post-SCI. (**D**) Percentage of pHrodo$^+$ macrophages at 1, 3 and 7 days post-SCI. (Two-way ANOVA followed by Bonferroni post-hoc test, $^*p \leq 0.05$). (**E, F**) Gating strategy and In vitro assay scheme of pHrodo-labeled myelin phagocytosis by BMDMs from WT and CD200R1$^{-/-}$ mice. (**G**) Quantification of the proportion of pHrodo$^+$ WT and CD200R1$^{-/-}$ BMDM in basal conditions and following 24 h of exposure to LPS (**H**) Quantification of pHrodo median fluorescence intensity in WT and CD200R1$^{-/-}$ BMDM in basal conditions and following 24 h of exposure to LPS. Each symbol represents one animal. Data are presented as mean ± SEM. For the in vitro experiments, each condition was performed in triplicate from cultures prepared from two independent animals per group (Two-way ANOVA followed by Bonferroni post-hoc test, $^*p \leq 0.05$, $^{***}p \leq 0.001$).

Peripheral blood immune response in CD200R1$^{-/-}$ mice after SCI

Inflammatory conditions are known to mobilize cells from the bone marrow and spleen altering cell numbers in blood[24,25]. Most spinal cord injuries (SCI) involve damage to surrounding tissues, including bone and muscle, in addition to the central nervous system (CNS). Thus, we included sham surgery for isolating the specific effects of CNS injury in some key experiments. First, we wanted to assess whether CD200R1$^{-/-}$ mice had similar blood cell counts that WT mice. No alterations in numbers of blood cells were observed under naïve conditions in most cell types between WT and CD200R1$^{-/-}$ mice, except for a lower lymphocyte count in mice lacking CD200R1 (Fig. 4A–D). The analysis of leukocyte cell populations in the bloodstream after either a Sham spinal cord surgery, where the spinal cord was exposed but not contused, or after a SCI revealed no significant impact of the absence of CD200R1 on the different cell types analysed (Fig. 4A–C).

To evaluate the systemic inflammatory response, the protein levels of relevant blood cytokines associated with the immune response following SCI were assessed in CD200R1$^{-/-}$ mice. While the SCI induced decreased circulating levels of IL23 and IL1a, it increased IL6 (Fig. 4D-G). The absence of CD200R1 had no significant effect on the blood cytokine levels in naive conditions nor at the different time points analysed after SCI (Fig. 4D–G). Taken together, these results show that the absence of CD200R1 had no impact on neither the numbers of the main circulating blood cells nor the main blood inflammatory cytokines after a local and systemic inflammatory condition such as SCI.

CD200R1 deficiency elicit spleen alterations in naïve conditions and after SCI

Since CD200R1$^{-/-}$ mice showed increased body weight loss after SCI, and the spleen is a critical organ in orchestrating and regulating the immune response following SCI[27], we investigated the consequences of CD200R1 deficiency in the splenic response to this inflammatory stimulus. Again, we first evaluated whether the absence of CD200R1 had any impact in the spleen weight. Surprisingly, under naïve conditions, CD200R1$^{-/-}$ mice exhibited a significant reduced spleen weight both in absolute terms (Suppl. Figure 5) and relative to body

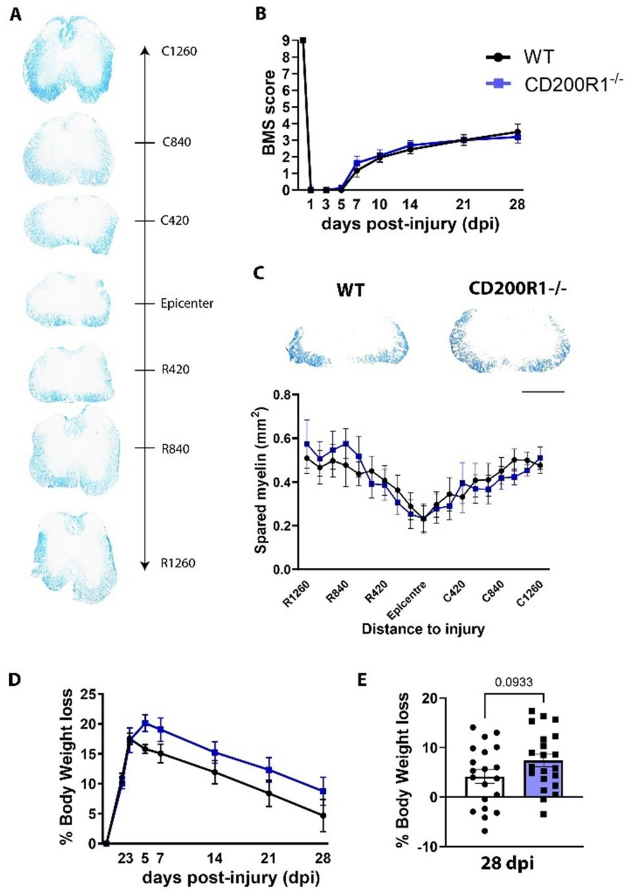

Fig. 3. Normal locomotor recovery and myelin loss after SCI in absence of CD200R1. (**A**) Representative images of Luxol Fast Blue stained sections at different distances rostrally and caudally to the epicentre of the lesion. (**B**) Functional recovery after SCI in WT and CD200R1$^{-/-}$ mice assessed by the BMS (Two-way ANOVA, genotype $p=0.92$, interaction $p=0.97$, Bonferroni post-hoc test; $n=9$ WT, $n=8$ CD200R1$^{-/-}$). (**C**) Quantification of preserved myelin area and representative images after 28 dpi calculated in Luxol Fast-Blue stained sections (Two-way ANOVA followed by Bonferroni post-hoc test; $n=6$ WT, $n=5$ CD200R1$^{-/-}$). (**D**) Percentage of body weight loss after SCI (Two-way ANOVA $p=0.1828$; $n=9$ WT, $n=8$ CD200R1$^{-/-}$). (**E**) Pooled data of the % weight loss of WT ($n=20$) and CD200R1$^{-/-}$ ($n=21$) at 28 dpi. Each symbol represents one animal. Data are presented as mean ± SEM. Statistical analysis: unpaired two-tailed t test, $p=0.09$.

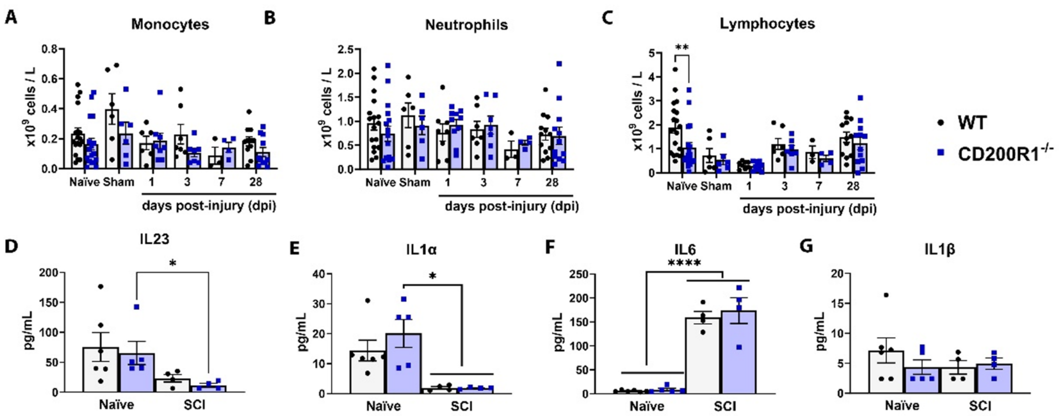

Fig. 4. Lower blood levels of lymphocytes in naïve conditions in absence of CD200R1. (**A–C**) Main blood leukocytes populations in naïve conditions, sham surgery and at different time points after SCI. (**A**) monocytes, (**B**) neutrophils, and (**C**) lymphocytes. (**D–G**) Blood cytokines levels in naïve conditions and acutely 24 h post-SCI. Each symbol represents one animal. Data are presented as mean ± SEM. Statistical analysis: Two-way ANOVA plus Bonferroni post-hoc test; *$p \leq 0.05$, **$p \leq 0.01$; ****$p \leq 0.001$.

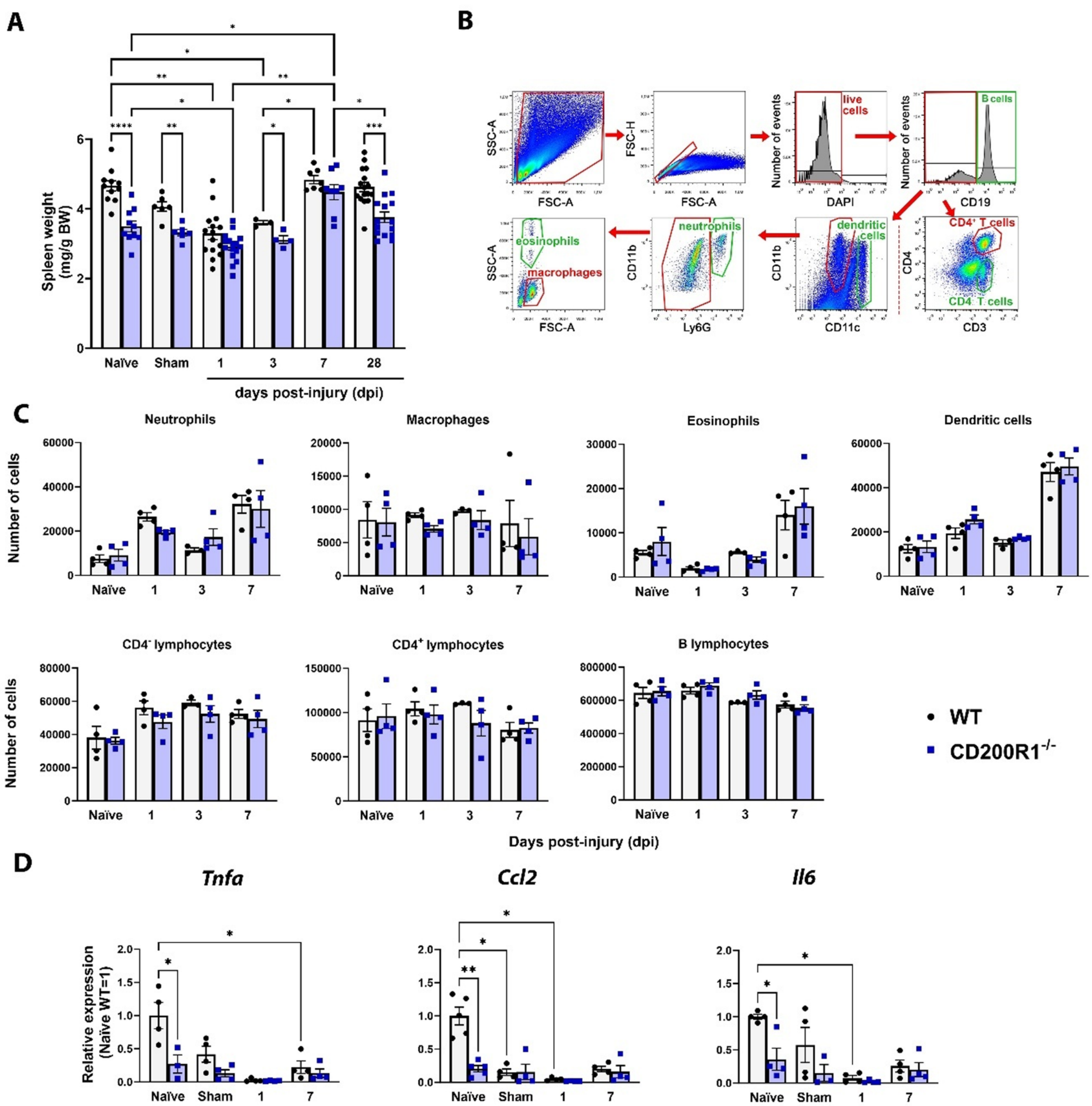

Fig. 5. Splenic atrophy in CD200R1$^{-/-}$ mice under naïve conditions and following SCI. (**A**) In naïve conditions, after a sham surgery, and 28 days after SCI, the spleen of CD200R1$^{-/-}$ has reduced weight normalized to body weight (BW) compared to the spleen of WT mice. (**B**) Representative flow cytometry dot blots of spleen. (**C**) Quantification of different cell populations in the spleen of naïve animals and after different time points after SCI. (**D**) QPCR of Tnfa, Ccl2 and Il6 in the spleen of naïve and sham surgery animals and at 1 and 7 days post-injury (dpi). Each symbol represents one animal. Data are presented as mean ± SEM. Statistical analysis: Two-way ANOVA followed by Bonferroni post-hoc test; $^{*}p \leq 0.05$, $^{**}p \leq 0.01$, $^{****}p \leq 0.0001$.

weight (BW) in comparison to WT mice (Fig. 5A), while no changes were observed in adult body weight (Suppl. Figure 5). Following SCI, WT mice underwent splenic atrophy at 1 dpi and 3 dpi, whereas such atrophy was not as pronounced after sham surgery. Conversely, CD200R1$^{-/-}$ mice exhibited splenic atrophy to a much lesser extent in response to the SCI, indicating a reduced splenic response in the absence of CD200R1. By 7 dpi, the spleen of WT mice regains its pre-SCI weight, whereas the spleen of CD200R1$^{-/-}$ mice exhibited a significant elevated weight compared to naïve values. By 28 dpi, spleen weights in both WT and CD200R1$^{-/-}$ mice were restored to naïve conditions maintaining the differences between genotypes observed (Fig. 5A).

To further understand the alterations in the response of the spleen to these inflammatory stimuli and the role of CD200R1 in this response, we analysed the main splenic immune cell populations after SCI (Fig. 5B). Although the spleen weight of CD200R1$^{-/-}$ mice was significantly lower in naïve conditions, the absence of CD200R1 had no significant impact on the number of any of the immune cell populations of the spleen analysed (Fig. 5C). Since the activation of CD200R1 downregulates the NFκB pathway[9,31], we then analysed the downstream NFκB genes Tnf-α, Ccl2 and Il6 in the naïve/sham spleen and after SCI. Surprisingly, the absence of CD200R1 induced decreased levels of the mRNA of all three genes in the spleen in homeostatic conditions without a significant impact after SCI (Fig. 5D). Taken together, these results suggest that CD200R1 is a central regulator of spleen biology under physiological conditions and in response to systemic DAMPs.

Discussion

Understanding the integrated inflammatory response of the organism and the role of immune receptors in this process in different organs is crucial for picturing a realistic view of the outcome of local and systemic inflammatory insults. We here undertook the quest to analyse the role of CD200R1 immune receptor in the regulation of local and systemic inflammatory responses against DAMPs produced after SCI. The absence of CD200R1 altered basal spleen weight and cytokine expression, and inhibited spleen reaction after SCI. At the local level, CD200R1 deficiency induced increased infiltration of macrophages after SCI and impairment of myelin phagocytosis both in vivo and in vitro.

SCI is considered a sterile inflammatory condition, as it arises in the absence of pathogens. Following SCI, DAMPs are released from injured tissues, triggering an inflammatory response[32]. SCI induces pronounced local inflammation due to the primary injury but also has systemic consequences, leading to acute secondary immunosuppression known as SCI-induced immune deficiency syndrome (SCI-IDS)[33]. It has been proposed that secondary immune organs, such as the spleen, may play a role in this syndrome.

The role of CD200R1 in neuroinflammatory conditions has been examined in various murine models of neuropathology. However, most studies have used CD200 knockout mice, even though CD200 can interact with receptors other than CD200R1, and CD200R1 itself may engage with ligands beyond CD200. Thus, studies using CD200 or CD200R1 knockouts are not equivalent.

In the present study we evaluated functional recovery after SCI in absence of CD2000R1. We performed a contusion injury at the lower thoracic level of the spinal cord and monitored the animals for 28 days, evaluating spontaneous functional recovery using the BMS scale. Previous results from our laboratory and others had found that blocking the CD200-CD200R1 interaction by using a blocking antibody against CD200R1 or a CD200-knockout mice, induced impaired functional recovery[21,22]. In contrast, our findings show no significant difference in BMS score between CD200R1-deficient and WT mice. These differences could be explained by compensatory mechanisms of other immune receptors when using knockout mice, by the existence of additional ligands for CD200R1 than CD200, or by CD200 activating other receptors.

When evaluating the recruitment of blood cells to the injured spinal cord parenchyma, we observed no differences in the acute infiltration of neutrophils. However, in the absence of CD200R1, there was a significant increase in the number of macrophages 24 h post-lesion, with a higher proportion of Ly6C$^+$ macrophages, indicating a more pro-inflammatory environment in CD200R1$^{-/-}$ mice. This aligns with findings by Ritzel et al., who reported an increase in microglia, Ly6C$^+$ macrophages, and lymphocytes after stroke in CD200R1$^{-/-}$ mice[20].

An important aspect following a SCI is the clearance of cellular debris and myelin from the injury site, which does not occur as efficiently as in the peripheral nervous system. This deficiency is linked to poorer functional recovery[34,35]. Myelin clearance primarily relies on the phagocytic activity of microglia and macrophages at the injury site. To date, few studies have investigated the role of CD200R1 in phagocytosis, and none have focused specifically on myelin phagocytosis; instead, previous research has examined its involvement in the phagocytosis of β-amyloid plaques in vitro[28] or in vivo[36], of tumor cells[37] or artificial stimuli such as beads[28]. Therefore, we set out to analyse myelin phagocytosis both in vitro and ex vivo, in the main cell populations responsible for carrying out this process following a CNS injury, namely microglia, macrophages, and to a lesser extent, neutrophils.

We analysed phagocytosis ex vivo by incubating the cells with myelin isolated from normal brain and conjugated with pHrodo immediately after tissue dissociation. This is a complementary approach to the classical in vitro analysis, where although with the limitations of phagocytosis occuring outside the organism and after a tissue dissociation procedure, the cells do not undergo the cell culture process, and thus may maintain a greater similarity to their in vivo characteristics. This approach also enables the analysis of phagocytosis across different cell populations. It has been previously suggested that in the early stages of the inflammatory response, microglia are primarily responsible for phagocytosing the debris of damaged tissue, while this role is mainly assumed by infiltrating macrophages a week post-injury[38]. In our study, we observed a similar trend in microglia, where myelin phagocytosis by this cell population decreased after the first day post-injury. However, this was not the case for macrophages, which exhibited higher phagocytic activity 24 h after SCI. The discrepancy between our findings and those of Greenhalgh and David could be attributed to methodological differences. Whereas Greenhalgh and David assessed the phagocytic capacity of both populations in vivo using fluorescent transgenic mice, our study involved isolated cells that may have already phagocytosed debris prior to analysis, and thus, the phagocytic performance by these cells could be changed. On the other hand, we observed that 24 h after SCI there was a significant decrease in the phagocytosis of myelin by macrophages lacking CD200R1 in comparison with WT. This difference was not observed neither microglia nor neutrophils. We aimed to further analyse the phagocytosis capabilities by using BMDMs of CD200R1$^{-/-}$ and WT mice. Again, BMDMs lacking CD200R1 exhibited a reduced capacity to phagocytose myelin, suggesting that CD200R1 plays an important role in myelin clearance. Further studies should be done in order to study the capacity of microglia and macrophages to phagocytose myelin isolated from spinal cord, instead of brain, but also myelin isolated from injured spinal cord. The analysis of preserved myelin at 28 dpi by Luxol Fast Blue staining showed no differences between WT and CD200R1$^{-/-}$ mice. This suggests that CD200R1 deficiency may delay myelin phagocytosis by macrophages following SCI but does not influence the level of myelin destruction. However, CD200R1 may affect the levels of myelin clearance over time and induce an accumulation of myelin debris, that could act as DAMPs and further stimulate inflammation, cell death and inhibit regeneration or plasticity.

Microglial cells express immune receptors as TREM2 or CD300f to recognize and engage the clearance of apoptotic cells[39,40]. Also, neurons express ligands which interact with the receptors expressed in the surface of microglia to engage don't eat me signals to maintain microglia in a homeostatic state and to continuously interact with neurons to monitor their functional status and homeostasis. Thus, by expressing CD200 or SIRPa, healthy neurons can control phagocytosis by microglia. However, in neurogenerative diseases, after a traumatic brain or spinal cord injury or after stroke, where death of neurons occurs, the lack of the 'don't eat me' signal can lead to enhanced phagocytosis of debris. Accordingly, it has been shown that the lack of CD200 both in constitutive knockout mice and in conditional neuronal or endothelial knockout mouse models, increases phagocytosis of fluorescent beads by microglial cells isolated from ischemic mice[28,41,42]. Interestingly, when using CD200R1$^{-/-}$ mice, they found similar results after stroke where mice lacking CD200R1 phagocytosed more fluorescent beads than WT mice[20]. Contrary to these results, in the present work we have observed a reduction in phagocytosis capability of myelin by macrophages lacking CD200R1. This inconsistency could be explained by differences in the experimental focus. While our work specifically examines the ability of microglia and macrophages to clear myelin, earlier studies have primarily assessed general phagocytic activity using fluorescent beads. Evaluating specific phagocytic activity is crucial, as the mechanisms involved can vary depending on the nature of the phagocytic target. For instance, LPS reduces apoptotic cell clearance by mouse peritoneal macrophages without affecting bead or yeast phagocytosis[30]. Additional research is required to explore the role of CD200R1 in myelin phagocytosis under demyelinating conditions and the further lipid processing.

As a result of a SCI, the autonomic innervation of the spleen is profoundly disrupted, an effect that becomes more pronounced with higher-level injuries[27,33]. This loss of control from higher neural centres leads to immune suppression, splenic atrophy, and impaired migration of splenic monocytes and lymphocytes to injured or affected organs, highlighting the critical role of this neuroimmune interface in shaping the immune response after SCI[43].

After SCI we observed that mice lacking CD200R1 showed a tendency towards losing more weight than WT counterparts. This fact led us to hypothesise that the lack of CD200R1 had a systemic effect beyond the spinal cord parenchyma. Interestingly, we uncovered a central role of CD200R1 in spleen biology under physiological conditions, as a significant reduction of spleen weight was observed, associated to a reduction of the mRNA for several important cytokines for spleen function such as Tnfa, Ccl2 and Il6. This was accompanied by a reduction in the numbers of circulating lymphocytes, but not of any other blood cell type analysed, nor in different resident immune cells of the spleen. The decrease in spleen weight in CD200R1$^{-/-}$ mice could be due to a different load of red blood cells in the red pulp, or other structural alterations. Regarding the decreased number of circulating lymphocytes, we have not analysed whether they were T or B lymphocytes, and thus this could be explained by alterations in bone marrow or thymus.

We also identified a role of splenic CD200R1 in the systemic response to SCI. After an injury, spleen atrophy occurs in both WT and CD200R1$^{-/-}$ mice, mainly due to apoptosis and the migration of cells into the bloodstream[44–46], returning to normal spleen weight by 7 dpi and maintaining differences between genotypes at long term (last time studied, 28 dpi). Unlike what is observed under normal conditions and in the sham laminectomy, the spleen weight of CD200R1$^{-/-}$ mice in the acute stages after injury is similar to that of WT mice. In the same direction, we did not observe differences in the number of macrophages, neutrophils, eosinophils, dendritic cells, and lymphocytes in the initial stages of the response to injury between CD200R1$^{/-}$ and WT mice.

These observations suggest that there are other factors influencing spleen weight besides the number of myeloid and lymphoid cells in the tissue. Among these factors, the number of erythrocytes in this organ is considerably high and can have a strong impact on spleen weight and may be one of the factors not analysed in this study that are determinant for the observed differences. On the other hand, these results suggest that the spleen in CD200R1$^{-/-}$ female mice is altered both in naïve conditions and after SCI, as both the changes observed in organ weight and the expression levels of the cytokines studied exhibit a different behaviour compared to WT mice.

This study has some limitations. We used a Cortical Impactor device, which lacks detailed output data like force and displacement, unlike the Horizon Impactor. Although we selected a reproducible contusion depth comparable to a 60 kdyn lesion from the Horizon device, such a strong injury may have masked potential differences in functional outcomes between wild-type and CD200R1-/- mice. Nevertheless, we took advantage of the similar CNS compromise observed between WT and CD200R1$^{-/-}$ mice, as this is important from the point of view of evaluating the effect of SCI on global immune reactions such as the one of the spleen. Finally, most experiments were conducted in female mice, with male data limited to spleen weight, so potential sex differences in CD200R1-related responses to SCI remain unexplored and thus we cannot rule out sex differences in SCI performance in absence of CD200R1.

Conclusions

Investigating the global response of the organism is highly relevant, as it could provide a deeper understanding of processes occurring outside the injury site that impact nervous tissue damage. This knowledge could lead to the development of less invasive and more precise therapeutic strategies for modulating the inflammatory response, thereby promoting better recovery following traumatic spinal cord injuries.

Methods

Animals

All surgical procedures and treatments described in this study received approval from the Institut Pasteur de Montevideo Animal Care Committee (approval number 005–19) and were conducted in strict accordance with international FELASA guidelines, Uruguayan national law, ethical guidelines set forth by the Uruguayan Animal Care Committee, and the ARRIVE guidelines for reporting animal research[47]. Adult (10–14 weeks old; 20–28 g of weight) CD200R1 wild type (WT) and CD200R1 knock-out (CD200R1$^{-/-}$) female mice were used in this study. The WT and CD200R1$^{-/-}$ (B6N.129S5-Cd200r1tm1Lex/Mmucd) mice were procured from the Mutant Mouse Resource and Research Centers at UC Davis in Davis, CA, USA. WT and CD200R1$^{-/-}$ mice were housed in separate cages, in a controlled environment with a 12-hour light-dark cycle and maintained at a temperature of 20 ± 1 ∘C, with a maximum of 6 mice per cage. WT and CD200R1$^{-/-}$ male mice were used in naïve conditions only to show comparisons in the body weight. At the end of the different studies, mice were euthanized by intraperitoneal injection of pentobarbitone (200 mg/kg), followed by transcardial perfusion either with ice-cold PBS or 4% Paraformaldehyde.

Spinal cord injury model

For the surgical procedure, female mice were anesthetized with ketamine (90 mg/kg, i.p) and xylazine (10 mg/kg, i.p). After performing a laminectomy at the 11th thoracic vertebrae, SCIs were performed using the PinPoint PCI3000 Precision Cortical Impactor (Hatteras Instruments) employing a 1 mm diameter piston. The impact parameters were set at a speed of 1.5 m/s with a spinal cord displacement of 1.2 mm. These conditions were based on initial experiments comparing 3 displacements (1, 1.2 and 1.5 mm; Suppl. Figure 1) and the follow up of locomotor recovery using the BMS scale. According to the clinical score obtained with the BMS scale and the spared myelin analyzed with Luxol Fast Blue staining (Fig. 3A, C) our conditions are equivalent to those obtained with the gold standard Horizon Impactor device settings of 60 Kdyn[48,49]. For the sham surgery, after performing the laminectomy at the 11th thoracic vertebrae, the wound was closed without impacting the spinal cord. Following complete recovery from anesthesia, mice received daily analgesic treatment with tramadol (5 mg/kg; i.p.) for 72 h post-injury. Animals were bladder expressed once per day until bladder control was recovered. Animals with a score higher than 1 in the BMS scale 24 h after injury, were excluded from the experiments.

Functional assessment

Locomotor recovery was assessed at various time points (1, 3, 5, 7, 10, 14, 21, and 28 days post-injury; dpi) using the nine-point Basso Mouse Scale (BMS)[50]. The BMS analysis of hindlimb movements and coordination was performed by two independent researchers blinded to the experimental groups and the consensus score was taken.

Hematology analysis

The number of white blood cells was quantified by the hematological analyzer Mindray-BC 5000 Vet from a blood sample of WT or CD200R1$^{-/-}$ mice under naïve conditions, and at 1, 3, 7 and 28 dpi. 18 µL of blood were collected from the right atrium into tubes with EDTA-2 K (1:10, Wiener Lab QC-1898552-W) after mice were deeply anesthetized and prior to intracardiac perfusion.

Blood cytokine assay

Blood samples from WT and CD200R1$^{-/-}$ mice in naïve conditions and 24 h following a SCI were collected from the left ventricle in a heparinized tube. Blood was centrifuged and quantification of IL-1 α, IL-1 β, IL-6 and IL-23 in serum was performed using the LEGENDplex Mouse Inflammation Panel (Biolegend 740446) following the manufacturer's protocol and acquired via BD Accuri C6 flow cytometry.

Flow cytometry

In naïve animals and at 1, 3,7 and 14 dpi (for lymphocytes analysis), mice were deeply anesthetized with Pentobarbitone (200 mg/kg; ip) and then perfused with ice-cold PBS to avoid interference between blood and parenchyma, and 6 mm of spinal cord tissue centered on the injury and/or the spleen were dissected out and weight. The tissue was cut into smaller pieces with scissors and incubated for 30 min at 37 °C for enzymatic disaggregation using 0.125% collagenase (Sigma C9407) and 0.125% DNase (Sigma D4527) in calcium- and magnesium-free PBS. Following digestion, the tissue was mechanically disaggregated through a 70 μm mesh, and the cell suspension in dissociation buffer (2% FBS, 0.1 M EDTA in PBS) was centrifuged. Each sample was then divided into tubes for antibody labeling or into a control tube without labeling to determine autofluorescence. The cells were incubated for 1 h at 4 °C with the antibody mixture. Cell suspension was then analyzed with the Attune NxT flow cytometer and FlowJo software. For phagocytosis assay, prior to labeling, the spinal cord tissue homogenates were incubated for 4 h at 37 °C with 3 µg of myelin conjugated to pHrodo according to Gomez-Lopez and colleagues[51].

The following antibodies were used to label cellular populations in the spinal cord according to[22,52]: CD45-eFluor405 (1:200, eBioscience 48–0451-82), CD11b-APC-Cy7 (1:100, Biolegend 101226), F4/80-PerCP-Cy5.5 (1:100 eBioscience 45–4801-82), Ly6G-PE (1:200, Biolegend 127608), Ly6C-FITC (1:100, Biolegend 128005), CD19-APC (1:100, Biolegend 152409) and CD4-PE (1:100, Biolegend 100408). Microglial cells were identified as CD45^{low} and CD11b^{+}, while other myeloid cells were identified as CD45^{high} and CD11b^{+} cells. Among those myeloid cells, neutrophils were identified as CD45^{high}, CD11b^{+}, Ly6G^{+} and macrophages were identified as CD45^{high}, CD11b^{+}, Ly6G^{-}, F4/80^{+}.

The following antibodies were used to label cellular populations in the spleen for population selection strategy according to[53]: CD11b-APC-Cy7 (1:100, Biolegend 101226), Ly6G-PE (1:200, Biolegend 127608), CD11c-FITC (1:100, Biolegend 117305), CD19-APC (1:100, Biolegend 152409), CD3-FITC (1:100, Biolegend 100204), CD4-PE (1:100, Biolegend 100408). DAPI was used to evidence dead cells. B cell population was identified as CD19^{+}, while CD4^{+} and CD4^{-} T cells were identified as CD19^{-}. Dendritic cells were identified as CD19^{+}, CD11c^{+} population. Neutrophil population was identified as CD19^{-}, CD11c^{-}, Ly6G^{+}. Eosinophils and macrophages were identified as CD19^{-}, CD11c^{-}, Ly6G^{-} and detected by high or low granularity (SSC), respectively.

Histology

At the end of the functional evaluation, mice were deeply anaesthetized with Pentobarbitone (200 mg/kg; ip) and perfused with 4% paraformaldehyde (PFA) in 0.1 M phosphate buffer (PB). A piece of 6 mm length of spinal cord containing the contusion site centered was harvested, postfixed with 4% PFA for 3 h, and cryoprotected with 30% sucrose in 0.1 M PB at 4 °C for a minimum of 48 h. The samples were cut on a cryostat (Leica) and 14-µm-thick transversal sections were picked up on glass slides, so adjacent sections on the same slide were 140 µm apart. After graded dehydration, sections were placed in a 1 mg/ml LFB solution in 95% ethanol and 0.05% acetic acid overnight at 37 °C. Sections were then washed in distilled water before being placed in a solution of 0.05% Li_2CO_3 for 30 s and a brief rinse in 70% Ethanol. After washing in distilled water, sections were dehydrated and mounted in DPX mounting media (Sigma). Image J software was used to perform the quantifications of spared myelin.

RNA isolation and QPCR

In naïve conditions and at 1 and 7 dpi, mice were deeply anesthetized with Pentobarbitone (200 mg/kg; ip) and then perfused with ice-cold PBS to remove blood. The spleen was harvested and split into half. One half was homogenized in Trizol (SIGMA, T9424), and the resulting aqueous phase was further purified using the Direct-zol RNA MiniPrep Plus kit (Zymo Research, R2070). RNA samples underwent reverse transcription using M-MLV reverse transcriptase (Invitrogen 28025-013) and random primers. Quantitative PCR (QPCR) was conducted utilizing TaqMan reagents from Invitrogen/Applied Biosystems: TaqMan Fast Advanced Master Mix (Invitrogen, 4444557) and probes for *Tnfa* (Mm00443258_m1), *Ccl2* (Mm00441242_m1) and *Il6* (Mm00446190_m1). Additionally, *Gapdh* endogenous control (Mm99999915_g1) was included in the model to standardize each reaction run in terms of RNA integrity and sample loading. QPCR was carried out using the QuantStudio 3 (Thermo-Fisher) Real-Time PCR System and software. The cycling conditions comprised 2 min at 50 °C, 2 min at 95 °C, followed by 40 cycles of 1 s at 95 °C and 20 s at 60 °C. The quantity of cDNA was determined based on the threshold cycle (CT) value and standardized by the amount of *Gapdh* using the $2^{-\Delta\Delta CT}$ method[54].

Myelin isolation and pHrodo conjugation

Myelin isolation and conjugation to pHrodo were performed in accordance with the methodology outlined by Gomez-Lopez et al.[51]. Briefly, brain homogenates from WT female mice of 12 weeks were obtained after enzymatic and mechanical disaggregation. Percoll was added to the brain homogenate and then layered between a Percoll phase of density 1.044 g/mL and PBS. Myelin was then obtained from the phase between the Percoll and the PBS. Subsequently, the protein quantification of the myelin was carried out using the bicinchoninic acid method according to Smith et al.[55] in a 96-well plate.

Once the myelin fraction was obtained, it was subjected to conjugation with pHrodo™ Green STP Ester (Invitrogen #P35369) reconstituted in DMSO. For conjugation, 277.5 µg of the purified myelin fraction in PBS at pH 8.0 was incubated with pHrodo for 45 min under agitation at room temperature. Subsequently, the mixture was centrifuged, and the pellet was resuspended PBS at pH 7.4 to achieve myelin conjugated to pHrodo with a final concentration of 0.3 µg/µL.

Phagocytosis analysis in bone marrow-derived macrophages (BMDM)

Bone marrow-derived macrophages (BMDM's) were isolated from 14-week-old WT and CD200R1$^{-/-}$ female mice, following established protocols. In brief, bone marrow cells were obtained by flushing the femur and tibia shafts with DMEM/F12 supplemented with 10% FBS and Penicillin/Streptomycin (complete DMEM/F12). These cells were cultured for five days in a 100 mm Petri dish with complete DMEM/F12 and 20 ng/mL recombinant mouse macrophage colony-stimulating factor protein (M-CSF, Biolegend #576406; San Diego, CA, USA), changing the medium after 3 days. Cells were subcultured at a density of 75,000 cells in 96-well cell culture plates using the same medium for an additional 3 days.

Following the differentiation of the precursors for 7 days, cells were incubated for 24 h with either lipopolysaccharide (LPS, 100 ng/mL; Sigma L2880) in complete DMEM/F12 with 20 ng/mL M-CSF or maintained in the same medium. Subsequently, the cells were incubated with 1.8 µg of myelin conjugated to pHrodo in complete DMEM/F12 medium with 5 ng/mL of M-CSF for 1 h. Finally, the cells were resuspended with trypsin for 30 min and analyzed using the Attune Nxt flow cytometer and FlowJo software for quantification. Prior to acquisition, cells were incubated with DAPI (1:1000, Sigma D9542) as a dead cell marker.

Data processing and statistical analysis

All graphical data, as well as the values indicated in the text are displayed as mean ± standard error of the mean (SEM). For statistical analyses comparing genotypes against another independent variable, a two-way ANOVA test followed by Bonferroni post-hoc test was employed. For experimental data with more than one experimental group and an independent variable, one-way ANOVA test followed by Bonferroni or Tukey post-hoc test was used. Student's two-tailed t-test was utilized for comparing mean differences between two experimental groups. A p-value ≤ 0.05 was considered statistically significant.

Data availability

All data generated in the current study are available from the corresponding author on reasonable request.

Received: 15 May 2025; Accepted: 15 October 2025
Published online: 20 November 2025

References

1. Wright, G. J. et al. Characterization of the CD200 receptor family in mice and humans and their interactions with CD200. *J. Immunol.* **171**, 3034–3046 (2003).
2. Akkaya, M., Aknin, M. L., Akkaya, B. & Barclay, A. N. Dissection of agonistic and blocking effects of CD200 receptor antibodies. *PLoS ONE* **8**, 85 (2013).
3. Wright, G. J. et al. Lymphoid/neuronal cell surface OX2 glycoprotein recognizes a novel receptor on macrophages implicated in the control of their function. *Immunity* **13**, 233–242 (2000).
4. Shrivastava, K., Gonzalez, P. & Acarin, L. The immune inhibitory complex CD200/CD200R is developmentally regulated in the mouse brain. *J. Comp. Neurol.* **520**, 2657–2675 (2012).
5. Meuth, S. G. et al. CNS inflammation and neuronal degeneration is aggravated by impaired CD200-CD200R-mediated macrophage Silencing. *J. Neuroimmunol.* **194**, 62–69 (2008).
6. Chitnis, T. et al. Elevated neuronal expression of CD200 protects Wlds mice from inflammation-mediated neurodegeneration. *Am. J. Pathol.* **170**, 1695–1712 (2007).
7. Hernangomez, M. et al. Brain innate immunity in the regulation of neuroinflammation: therapeutic strategies by modulating CD200-CD200R interaction involve the cannabinoid system. *Curr. Pharm. Design.* **20**, 4707–4722 (2014).
8. Mihrshahi, R., Barclay, A. N. & Brown, M. H. Essential roles for Dok2 and RasGAP in CD200 Receptor-Mediated regulation of human myeloid cells. *J. Immunol.* **183**, 4879–4886 (2009).
9. Mihrshahi, R. & Brown, M. H. Dok1 and Dok2 play opposing roles in CD200R signaling. *J. Immunol. (Baltimore Md. : 1950)*. **185**, 7216–7222 (2010).
10. Petermann, K. B. et al. CD200 is induced by ERK and is a potential therapeutic target in melanoma. *J. Clin. Invest.* **117**, 3922–3929 (2007).
11. Nip, C., Wang, L. & Liu, C. CD200/CD200R: Bidirectional role in cancer progression and immunotherapy. *Biomedicines* **11**, (2023).
12. Gorczynski, R. M., Yu, K. & Clark, D. Receptor engagement on cells expressing a ligand for the Tolerance-Inducing molecule OX2 induces an immunoregulatory population that inhibits alloreactivity in vitro and in vivo. *J. Immunol.* **165**, 4854–4860 (2000).
13. Gorczynski, R. M., Chen, Z., Kai, Y., Wong, S. & Lee, L. Induction of tolerance-inducing antigen-presenting cells in bone marrow cultures in vitro using monoclonal antibodies to CD200R. *Transplantation* **77**, 1138–1144 (2004).
14. Koning, N., Swaab, D. F., Hoek, R. M. & Huitinga, I. Distribution of the immune inhibitory molecules CD200 and CD200R in the normal central nervous system and multiple sclerosis lesions suggests neuron-glia and glia-glia interactions. *J. Neuropathol. Exp. Neurol.* **68**, 159–167 (2009).
15. Manich, G. et al. Role of the CD200-CD200R axis during homeostasis and neuroinflammation. *Neuroscience* **405**, 118–136 (2019).
16. Deczkowska, A., Amit, I. & Schwartz, M. Microglial immune checkpoint mechanisms. *Nat. Neurosci.* **21**, 779–786 (2018).
17. Hoek, R. H. et al. Down-regulation of the macrophage lineage through interaction with OX2 (CD200). *Science* **290**, 1768–1771 (2000).
18. Liu, Y. et al. CD200R1 agonist attenuates mechanisms of chronic disease in a murine model of multiple sclerosis. *J. Neurosci.* **30**, 2025–2038 (2010).
19. Cox, F. F., Carney, D., Miller, A., Lynch, M. A. CD200 fusion protein decreases microglial activation in the hippocampus of aged rats. *Brain. Behav. Immun.* **26**, 789–796 (2012).
20. Ritzel, R. M. et al. CD200-CD200R1 inhibitory signaling prevents spontaneous bacterial infection and promotes resolution of neuroinflammation and recovery after stroke. *J. Neuroinflamm.* **16**, 1–16 (2019).
21. Cohen, M. et al. Newly formed endothelial cells regulate myeloid cell activity following spinal cord injury via expression of CD200 ligand. *J. Neurosci.* **37**, 972–985 (2017).
22. Lago, N., Pannunzio, B., Amo-Aparicio, J., López-Vales, R. & Peluffo, H. CD200 modulates spinal cord injury neuroinflammation and outcome through CD200R1. *Brain. Behav. Immun.* **73**, 416–426 (2018).
23. Pannunzio, B. et al. CD200R1 contributes to successful functional reinnervation after a sciatic nerve injury. *Cells* **11**, 1–16 (2022).
24. Bronte, V. & Pittet, M. J. The spleen in local and systemic regulation of immunity. *Immunity* **39**, 806–818 (2013).
25. Milich, L. M., Ryan, C. B. & Lee, J. K. The origin, fate, and contribution of macrophages to spinal cord injury pathology. *Acta Neuropathol.* **137**, 785–797 (2019).
26. Blomster, L. V. et al. Mobilisation of the Splenic monocyte reservoir and peripheral CX3CR1 deficiency adversely affects recovery from spinal cord injury. *Exp. Neurol.* **247**, 226–240 (2013).
27. Noble, B. T., Brennan, F. H. & Popovich, P. G. The spleen as a neuroimmune interface after spinal cord injury. *J. Neuroimmunol.* **321**, 1–11 (2018).
28. Lyons, A. et al. Analysis of the impact of CD200 on phagocytosis. *Mol. Neurobiol.* **54**, 5730–5739 (2017).
29. Regen, T. et al. CD14 and TRIF govern distinct responsiveness and responses in mouse microglial TLR4 challenges by structural variants of LPS. *Brain. Behav. Immun.* **25**, 957–970 (2011).
30. Feng, X. et al. Lipopolysaccharide inhibits macrophage phagocytosis of apoptotic neutrophils by regulating the production of tumour necrosis factor α and growth arrest-specific gene 6. *Immunology* **132**, 287–295 (2011).
31. Sun, H. et al. The CD200 / CD200R signaling pathway contributes to spontaneous functional recovery by enhancing synaptic plasticity after stroke. 1–15 (2020).
32. Relja, B. & Land, W. G. Damage-associated molecular patterns in trauma. *Eur. J. Trauma Emerg. Surg.* **46**, 751–775 (2020).
33. Brommer, B. et al. Spinal cord injury-induced immune deficiency syndrome enhances infection susceptibility dependent on lesion level. *Brain* **139**, 692–707 (2016).
34. Van Broeckhoven, J., Sommer, D., Dooley, D., Hendrix, S. & Franssen, A. J. P. M. Macrophage phagocytosis after spinal cord injury: when friends become foes. *Brain* **144**, 2933–2945 (2021).
35. Bellver-Landete, V. et al. Microglia are an essential component of the neuroprotective scar that forms after spinal cord injury. *Nat. Commun.* **10**, 78 (2019).
36. Varnum, M. M., Kiyota, T., Ingraham, K. L., Ikezu, S. & Ikezu, T. The anti-inflammatory glycoprotein, CD200, restores neurogenesis and enhances amyloid phagocytosis in a mouse model of alzheimer's disease. *Neurobiol. Aging*. **36**, 2995–3007 (2015).
37. Li, J. et al. CD200R1-CD200 checkpoint inhibits phagocytosis differently from SIRPα-CD47 to suppress tumor growth. *Nat. Commun.* **16**, 96 (2025).
38. Greenhalgh, A. D. & David, S. Differences in the phagocytic response of microglia and peripheral macrophages after spinal cord injury and its effects on cell death. *J. Neurosci.* **34**, 6316–6322 (2014).
39. Takahashi, K., Rochford, C. D. P. & Neumann, H. Clearance of apoptotic neurons without inflammation by microglial triggering receptor expressed on myeloid cells-2. *J. Exp. Med.* **201**, 647–657 (2005).
40. Negro-demontel, M. L., Evans, F., Cawen, A. & Fitzpatrick, Z. CD300f immune receptor is a microglial tissue damage sensor and regulates efferocytosis after brain damage. (2024).
41. Al Mamun, A. et al. Neuronal CD200 signaling is protective in the acute phase of ischemic stroke. *Stroke* **52**, 3362–3373 (2021).
42. Misrani, A. et al. Brain endothelial CD200 signaling protects brain against ischemic damage. *Brain Res. Bulletin* **207**, 85 (2024).
43. Iversen, P. O. et al. Depressed immunity and impaired proliferation of hematopoietic progenitor cells in patients with complete spinal cord injury. *Blood* **96**, 2081–2083 (2000).
44. Huston, J. M. et al. Cholinergic neural signals to the spleen Down-Regulate leukocyte trafficking via CD11b. *J. Immunol.* **183**, 552–559 (2009).

45. Seifert, H. A. et al. A transient decrease in spleen size following stroke corresponds to splenocyte release into systemic circulation. *J. Neuroimmune Pharmacol.* **7**, 1017–1024 (2012).
46. Prüss, H. et al. Spinal cord injury-induced immunodeficiency is mediated by a sympathetic-neuroendocrine adrenal reflex. *Nat. Neurosci.* **20**, 1549–1559 (2017).
47. Kilkenny, C., Browne, W. J., Cuthill, I. C., Emerson, M. & Altman, D. G. Improving bioscience research reporting: the arrive guidelines for reporting animal research. *PLoS Biol.* **8**, 6–10 (2010).
48. Francos-Quijorna, I. et al. Maresin 1 promotes inflammatory resolution, neuroprotection, and functional neurological recovery after spinal cord injury. *J. Neurosci.* **37**, 11731–11743 (2017).
49. Coll-Miró, M. et al. Beneficial effects of IL-37 after spinal cord injury in mice. *Proc. Natl. Acad. Sci. U.S.A.* **113**, 1411–1416 (2016).
50. Basso, D. M. et al. Basso mouse scale for locomotion detects differences in recovery after spinal cord injury in five common mouse strains. *J. Neurotrauma*. **23**, 635–659 (2006).
51. Gómez-López, A. R. et al. Evaluation of Myelin phagocytosis by Microglia/Macrophages in nervous tissue using flow cytometry. *Curr. Protocols.* **1**, 1–18 (2021).
52. Amo-Aparicio, J., Martínez-Muriana, A. & Sánchez-Fernández, A. López-Vales, R. Neuroinflammation quantification for spinal cord injury. *Curr. Protocols Immunol.* **123**, 1–15 (2018).
53. Rose, S., Misharin, A. & Perlman, H. A novel Ly6C/Ly6G-based strategy to analyze the mouse Splenic myeloid compartment. *Cytometry Part. A*. **81 A**, 343–350 (2012).
54. Livak, K. J. & Schmittgen, T. D. Analysis of relative gene expression data using real-time quantitative PCR and the 2-ΔΔCT method. *Methods* **25**, 402–408 (2001).
55. Smith, P. K. et al. Measurement of protein using bicinchoninic acid. *Anal. Biochem.* **150**, 76–85 (1985).

Acknowledgements
We thank the Laboratory Animals Biotechnology Unit, the Cell Biology Unit and the Advanced Bioimaging Unit of the Institut Pasteur de Montevideo for their support and assistance in the present work.

Author contributions
NL, BP, and HP conceived the study. BP, CA, FE and NL performed the experiments. BP, HP, RLV and NL analysed and discussed results. BP and NL drafted the original manuscript and RLV and HP contributed to the edition of the final version. All authors read and approved the final manuscript.

Funding
This work was supported by Ministerio de Ciencia, Innovación y Universidades, la Agencia y del Fondo Europeo de Desarrollo Regional (proyecto PID2023-146560OB-I00 and proyecto PID2023-152474OB-I00 funded by MCIU/AEI/10.13039/501100011033 and by FEDER/UE) to NL and RLV, as well as by RICORS-Terav (RD24/0014/0001) funded by Instituto de Salud Carlos III and co-funded by EU. This work has been supported by grants from Comisión Sectorial de Investigación Científica (CSIC-UDELAR), Uruguay; PEDECIBA, Uruguay; FOCEM (MERCOSUR Structural Convergence Fund), COF 03/1111; and Banco de Seguros del Estado (BSE), Uruguay; Marie Sk1odowska-Curie Individual Fellowship (H2020-MSCAIF-2020 no. 101030280) to NL.

Declarations

Competing interests
The authors declare no competing interests.

Additional information
Supplementary Information The online version contains supplementary material available at https://doi.org/10.1038/s41598-025-24827-6.

Correspondence and requests for materials should be addressed to N.L.

Reprints and permissions information is available at www.nature.com/reprints.

Publisher's note Springer Nature remains neutral with regard to jurisdictional claims in published maps and institutional affiliations.